

**Gross Error Detection:
Maximising the Use of Data with UBA on Global Producer III (Part 2)**

**Neil Corbett, Maersk
Robert Sibbald, Accord
Phillip Stockton, Accord
Allan Wilson, Accord**

1 INTRODUCTION

Validation of input data and results is a key component of all allocation workflows and applies to a variety of data: metered quantities, well estimates, component fractions, plant operating conditions, and allocation results. Data validation is addressed throughout the length of the allocation data chain by different stakeholders and by a variety of means. Allocation computer systems are no exception: they normally include validation packages as standard and typically alert users when data or calculated results are, for example, missing, stuck, or lie outside an expected range. Some of the test thresholds can seem arbitrary. This need not be the case; knowledge of the uncertainties in an allocation system's input data can be utilised in rigorous statistical tests based on conservation laws and data reconciliation.

In a previous paper [1] we presented a non-linear uncertainty based allocation method for Maersk's GPIII FPSO serving the Dumbarton and Lochranza fields. In this paper we demonstrate several gross error detection techniques for validating GPIII input data and allocation results based on statistical tests adopted from linear data reconciliation. The gross error tests are natural extensions to GPIII's non-linear uncertainty based allocation method.

Though the statistical tests are rigorously derived for the linear case we demonstrate the ability to detect the location and size of gross errors in non-linear data reconciliation through Monte Carlo simulation and investigate their performance when applied to real field data.

Data reconciliation has been an active area of research since the mid-1960s [2] and has been applied in the chemical, power and oil and gas industries to name a few. However its use remains uncommon in the UKCS, and North Sea in general. Some examples are published in [3],[4],[5]. Data reconciliation provides an optimal estimate of process variables consistent with physical constraints, such as conservation of mass and energy, but is reliant on the input process variables being subject to random errors only. Any gross errors in the input variables will skew the results away from their true optimal values.

The intent of this paper is to highlight some of the statistically rigorous gross error detection (GED) tests which extend data reconciliation beyond simply providing allocation results. We do this through studying a simple fictitious allocation system, and Maersk's GPIII Uncertainty Based Allocation system. In doing so, we hope to show that GED techniques are not only a natural extension for allocation systems utilising data reconciliation techniques, but that with a little extra information on

measurement uncertainties some of the tests can be applied to more traditional pro-rata based allocation systems.

In Section 2, the concepts and tests used for gross error detection in the rest of the paper are introduced. Section 3 describes the use of Monte Carlo techniques to demonstrate a variety of GED tests when applied to a simple fictitious allocation system. From here the focus turns to GPIII with Section 4 describing the subsea configuration and topsides process, along with the uncertainty-based allocation system presented in the previous paper [1]. Section 5 demonstrates the outcome of applying GED tests to GPIII's non-linear uncertainty-based allocation system. The results of the gross error detection tests when applied to a selection of real GPIII production data are presented in Section 6 and conclusions are provided in Section 7. For the interested reader, Section 8 contains mathematical detail regarding the uncertainty-based allocation calculations.

.

2 CONCEPTS

Before introducing and implementing gross error detection techniques it is worthwhile explaining concepts used throughout this feasibility study.

2.1 Random Errors and Gross Errors

Random errors are ever present in oil and gas measurements, caused by small changes in ambient conditions. These random errors result in imbalances in physical conserved quantities such as mass and energy across processing facilities. Since the mid-1960s data reconciliation techniques have been developed to deal with the random errors and enable the best estimate of true measurement values to be obtained from actual measurements subject to physical conservation laws, based on rigorous mathematical and statistical techniques.

Gross errors can arise in oil and gas measurements if a meter is miscalibrated, poorly maintained, damaged, operated outside its certified regime or fouled. In a steady-state production environment a gross error will manifest itself as a sudden change or as a drift over time in a measured value from the steady-state value. A great deal of effort has been spent and continues to be spent implementing and developing standards and tools to ensure measurement data quality. This varies from regular meter inspection, auditing and calibration of metering packages, online diagnostic checks in flow meters or additional diagnostic packages to data quality checks in allocation systems. Yet all this effort is no guarantee of data quality. As was reported in [6] errors may arise in the allocation workflow where there are many links between an initial data source, be it meter or well production estimate and the allocation computer system.

Gross errors will skew allocation results away from the correct results, and if undetected for a long period of time can result in misallocations worth millions of Dollars, reputational damage, not to forget the time and effort lost to corrective work.

2.2 Confidence Levels and Gross Error Tests

For the purposes of this paper it is assumed that all measurements are normally distributed about a true value, μ , with a standard deviation, σ . Based on the properties of the normal distribution we could reject any new measurement more than 2σ different from the mean with 95% confidence. Or put another way, at the 95% Confidence Level the new measurement is not consistent with the mean.

In the tests that follow, rather than directly comparing measurements to a hypothetical mean and standard deviation of a Gaussian distribution, calculations will be used to derive a test statistic upon which gross errors in the measurements can be detected. The test statistics all make use of the same idea of a confidence level, which will be evaluated based on either a Gaussian or Chi-squared (χ^2) distribution, depending on the details of the test.

The choice of Confidence Level is arbitrary, but affects the outcome of Gross Error tests. If the confidence level is set too low, gross errors may be detected when none exist; the test has raised a false alarm and is said to have committed a Type 1 error. If the confidence level is set too high, gross errors are not detected when one or more

exist; the test is said to have committed a Type 2 error. If we denote the Type 2 Error rate of a test as, θ , then the ‘Power’ of a statistical test is defined as,

| | |
|----------------------|-----|
| $Power = 1 - \theta$ | [1] |
|----------------------|-----|

When setting the confidence level at which to identify gross errors there is a trade-off between the Type 1 Error rate (the probability of raising a false alarm) and Power (the probability of correctly identifying gross errors when they exist). A confidence level of 95% has been used throughout this paper.

Three different tests are used in this paper for identifying gross errors:

- 1- Allocation Factors;
- 2- Global Test;
- 3- Generalised Likelihood Ratio (GLR) Test.

Allocation Factors are routinely used in allocation systems as a data quality check. Defined as the ratio of allocated to measured mass (after accounting for shrinkage) for a field or well Allocation Factors are typically expected to be about 1. A margin of uncertainty for Allocation Factors could be determined analytically or by Monte Carlo means for any system, but in reality often seemingly arbitrary margins of 5, 10 or 20% are applied.

The Global Test and GLR Test are standard GED tests from data reconciliation literature. Detailed definitions of the tests are given in sections 3 and 5 where they are used. They are a natural extension to the data reconciliation approach used in the GPIII allocation system. These are some of the simplest tests available for gross error detection documented in [5] and references therein.

The Global test enables data to be tested for the presence of gross errors but does not identify the erroneous measurement(s) without further effort. The GLR Test enables the presence of gross errors to be detected and in theory the erroneous measurement to be identified. It also has the additional benefit of enabling the size of a single gross error to be estimated and therefore applied as a correction to the input data. It has been shown theoretically that if there is at most a single gross error in a system then the GLR test has the maximum power, compared to other tests not reviewed in this paper (Constraint Test, Maximum Power Constraint Test, Measurement Test and Maximum Power Measurement Test). Although not included in this study, the GLR test can also be used to identify unknown leaks in a system.

GED tests have been derived for systems subject to linear constraints in the process variables and operating in steady-state. For the GPIII system considered here the gas mass constraints are nonlinear (actually bilinear as they contain a term which is a product of two quantities to be reconciled). This analysis uses the gross error tests under the assumption that the non-linearity effects will either be small or will be identified through the simulation studies. The assumption of a steady-state operating system is often not valid in reality and the effects of this will be seen in analysing the

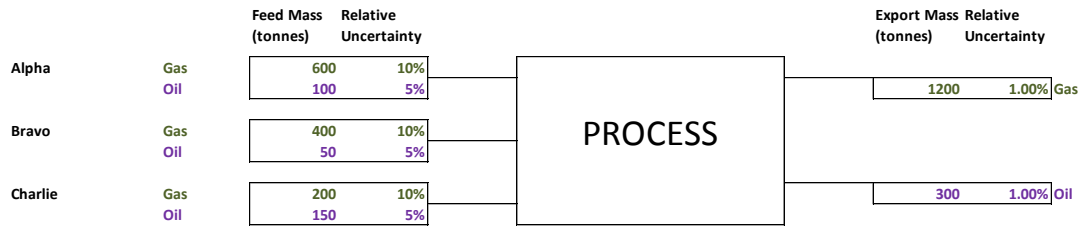
33rd International North Sea Flow Measurement Workshop
20th – 23rd October 2015

actual GPIII data. The success, or otherwise, of the tests are examined under these conditions.

3 SIMPLE LINEAR ALLOCATION SYSTEM EXAMPLE

A demonstration of the gross error tests used in this paper is provided using a simple fictitious example system consisting of three fields, Alpha, Bravo and Charlie. The produced hydrocarbons from the three fields are commingled and processed to produce export gas and export oil. All streams are assumed to be metered. The process, assumed feed and export stream masses and measurement uncertainties are shown in Figure 1. The example is very contrived having no shrinkage and perfect mass balance! Export Oil and Gas are allocated back to Alpha, Bravo and Charlie pro-rata to their measured mass.

Figure 1 - The simple linear allocation system used to demonstrate GED tests



3.1 Test Definitions

For the GED tests used in this paper it is necessary to define the constraints applicable to this process:

$$-m_{Export,Oil} + m_{Alpha,Oil} + m_{Bravo,Oil} + m_{Charlie,Oil} = 0 \quad [2]$$

$$-m_{Export,Gas} + m_{Alpha,Gas} + m_{Bravo,Gas} + m_{Charlie,Gas} = 0 \quad [3]$$

We define y to be a vector of measured data such that

$$y = \begin{bmatrix} m_{Export,Oil} \\ m_{Export,Gas} \\ m_{Alpha,Oil} \\ m_{Alpha,Gas} \\ \vdots \\ m_{Charlie,Gas} \end{bmatrix} \quad [4]$$

and a Constraint matrix, A , which contains one row for each constraint applicable to the process. In any row the entries in a column are +1 for any stream flowing into the process, -1 for any stream exiting the process, and 0 for any stream which is not involved in the constraint. The columns of A are ordered identically to the rows in the measured data vector, y .

Thus the Constraint matrix for the above process can be written as

$$A = \begin{bmatrix} -1 & 0 & 1 & 0 & 1 & 0 & 1 & 0 \\ 0 & -1 & 0 & 1 & 0 & 1 & 0 & 1 \end{bmatrix} \quad [5]$$

The first row of A represents the oil mass balance and the second row the gas mass balance across the system. The physical constraints applicable to the system can then be written succinctly as,

$$Ay = 0 \quad [6]$$

Uncertainties in each measurement are assumed to be independent of one another thus their Covariance matrix, V , is diagonal, with each stream's entry on the main diagonal calculated from its mass, m , and relative uncertainty, ε , as $\left(\frac{m \cdot \varepsilon}{2}\right)^2$.

Allocation Factor

For this simple example where product is allocated pro-rata to each field's production the Oil Allocation Factor for oil will be

$$AF_{Oil} = \frac{m_{Export,Oil}}{m_{Alpha,Oil} + m_{Bravo,Oil} + m_{Charlie,Oil}} \quad [7]$$

The Gas Allocation Factor is calculated analogously. We will assume an Allocation Factor in the range $0.9 < AF < 1.1$ is acceptable for both oil and gas, thus $AF < 0.9$ or $AF > 1.1$ would signal the presence of a gross error.

Global Test

The Global test uses the test statistic calculated from the matrices defined above

$$\gamma = Ay(AVA^T)^{-1}(Ay)^T = r^T \Sigma^{-1} r \quad [8]$$

where the constraint residual vector $r = (Ay)^T$ represents the amount of violation of each constraint and the Covariance matrix $\Sigma = AVA^T$ represents the uncertainty in each constraint.

Under the null hypothesis (that the data are free of gross errors) the above statistic follows a χ^2 distribution with 2 degrees of freedom (one per constraint). A gross error is detected if $\gamma \geq \chi^2(\alpha)$, for the chosen confidence level, α . At a 95% confidence level, a gross error is detected if $\gamma \geq 5.99$.

Generalised Likelihood Ratio Test

The GLR Test is calculated from the constraint residual vector $r = (Ay)^T$ as used in the Global Tests. The test establishes which is more likely; the null hypothesis that there is no gross error in the input data, or an alternative hypothesis, that there is one or more gross errors in the input data.

For each measurement the test statistic is calculated as:

$$T_k = \frac{d_k^2}{C_k} \quad [9]$$

where

$$d_k = f_k^T (A V A^T)^{-1} r = f_k^T \Sigma^{-1} r \quad [10]$$

$$C_k = f_k^T (A V A^T)^{-1} f_k = f_k^T \Sigma^{-1} f_k \quad [11]$$

and each vector f_k is the column of the Constraint matrix corresponding to the measurement.

Under the null hypothesis the above statistic follows a χ^2 distribution with 1 degree of freedom. As explained in [8], to reduce the probability of a false-alarm (Type 1 error) due to multiple applications of a univariate test, a modified confidence level is used and a gross error is detected if any of the test statistics exceed the test criterion $\chi^2(\beta)$ where

$$\beta = 1 - (1 - \alpha)^{1/m} \quad [12]$$

α is the chosen confidence level and m is the number of measurements. This reduced confidence level ensures that the Type I error rate is at most α .

For the purposes of this study, gross errors were detected at a 95% confidence level. This equates to setting $\alpha = 0.05$ and with 8 measurements, $\beta = 0.006$. A gross error is then detected if any of the measurement test statistics, $\chi^2(\beta) \geq 7.44$.

For the measurement with the highest test statistic above the threshold, the GLR test allows the error on that measurement to be estimated as

$$b_k = \frac{d_k}{C_k} \quad [13]$$

3.2 Monte Carlo Simulation

A Monte Carlo (MC) simulation approach has been taken to demonstrate the expected outcomes of each of the gross error tests. Two separate simulation runs each with 100,000 trials were generated.

In the first simulation run production and export stream masses were generated from normal distributions with mean and standard deviation given by the masses and uncertainties in Figure 1 without gross errors. From this simulation each test's Average Type 1 Error rate (AVTI) can be established as,

$$AVTI = \frac{\text{Number of false alarms}}{\text{Number of trials}} \quad [14]$$

In the second simulation run the sign and magnitude of a gross error of between 5 and 10 standard deviations were generated at random from a uniform distribution then applied to one randomly selected stream in each trial. From this simulation each test's Power can be calculated as,

$$\text{Power} = \frac{\text{Number of gross errors correctly identified}}{\text{Number of gross errors simulated}} \quad [15]$$

In this analysis the number of gross errors simulated is the same as the number of trials.

Allocation Factors

Figure 2 shows the probability density ¹distribution of the Oil and Gas Allocation Factors from the simulation with gross errors. (For simplicity in the rest of the paper we will refer to probabilities or probability distributions rather than probability density.)

Both distributions have large peaks about the value 1. These peaks are due to the random variation in the Oil Allocation Factor for trials where the gross error was simulated in a gas measurement and vice-versa.

The chosen acceptable range $0.9 < AF < 1.1$ is delimited by the vertical red lines. The Oil Allocation Factor has a narrower distribution than the Gas Allocation Factor reflecting the lower uncertainties assumed on the oil streams and suggesting it is less sensitive to gross errors of the magnitude simulated.

¹ Probability density is defined as the fraction of trials with an Allocation Factor in a bin of the histogram relative to the total number of trials, divided by the width of the bin. Thus the total area depicted in the figures is 1.

Figure 2 - Distribution of Oil and Gas Allocation Factor from MC simulation with gross errors.

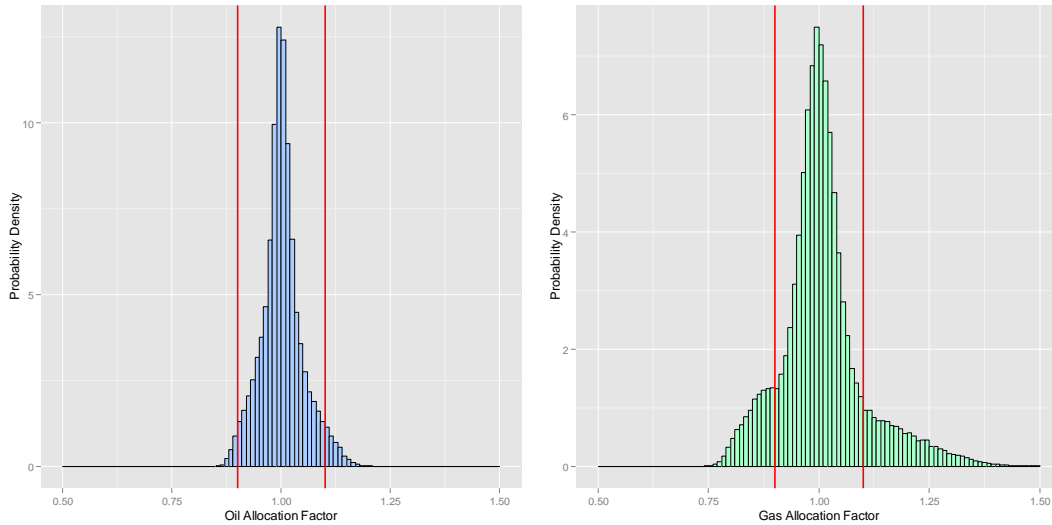


Figure 3 shows the same Oil and Gas Allocation Factor distributions, according to gross error location. Oil Allocation Factors are shown only for trials where the gross error is located in the associated oil stream, and likewise for the Gas Allocation Factor. The distributions therefore do not contain the trials with an Oil or Gas Allocation Factor about 1, which form the central peaks in Figure 2. The results of simulations with positive and negative valued gross errors are shown on the same plots; this leads to the distributions having two peaks. Allocation Factors less than 1 arise when the gross error is an over-reading, and these errors give a narrower peak when compared to gross under-readings

Figure 3 - Distribution of Oil and Gas Allocation Factors from MC simulation with gross errors according to location.

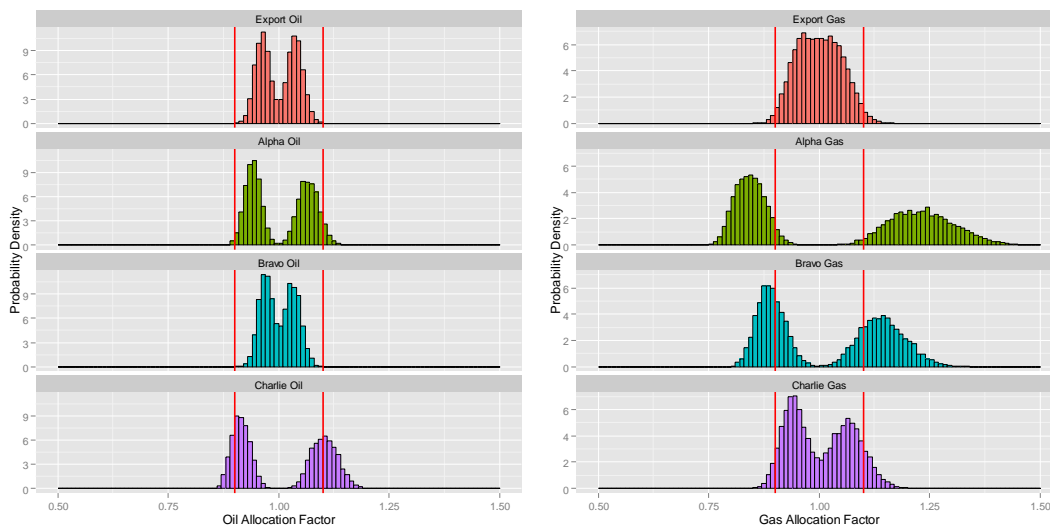


Figure 3 demonstrates the Oil Allocation Factor is fairly insensitive to gross errors. Except for Charlie's Oil Allocation Factor, the results suggest tests based on the Oil Allocation Factor would be insensitive to gross errors of the size simulated, and choice of acceptable range. Figure 3 also demonstrates the differing sensitivity of the Gas Allocation Factor according to location of the gross error. The Gas Allocation

Factor is most sensitive to a gross error on Alpha, followed by Bravo then Charlie. There is no or little sensitivity to gross errors in the export streams. The order reflects the stream flow rates and measurement uncertainties assumed in this example.

Table 1 quantifies the performance of the Oil and Gas Allocation Factor test demonstrated in Figure 3 according to the test's AVTI and Power. The first two columns report the performance irrespective of the gross error location; subsequent columns indicate the simulated gross error's location

Table 1 – Allocation Factor test performance statistics.

| Allocation Factor Error Location | Oil Overall | Gas Overall | Oil Export Oil | Gas Export Gas | Oil Alpha Oil | Gas Alpha Gas | Oil Bravo Oil | Gas Bravo Gas | Oil Charlie Oil | Gas Charlie Gas |
|-------------------------------------|----------------|----------------|----------------------|----------------------|------------------|---------------------|------------------|---------------------|-----------------------|-----------------------|
| Type I Error | 0.000 | 0.002 | 0.000 | 0.002 | 0.000 | 0.002 | 0.000 | 0.001 | 0.000 | 0.002 |
| Power | 0.055 | 0.233 | 0.000 | 0.029 | 0.051 | 0.964 | 0.000 | 0.717 | 0.397 | 0.132 |

AVTI is very low for all streams irrespective of gross error location. The Allocation Factor test is exceedingly unlikely to generate a false alarm. However the test's Power reveals a different tale; its ability to identify a gross error is strongly subject to the location, and for the most part, poor.

Global Test

The Global Test statistic probability distribution from the simulation with gross errors is depicted in Figure 4 and according to gross error location in Figure 5. The red vertical line denotes the critical test threshold, the 95% confidence level above which a gross error is detected, $\gamma \geq 5.99$

Figure 4 - Distribution of Global Test Statistic from MC simulation with gross errors.

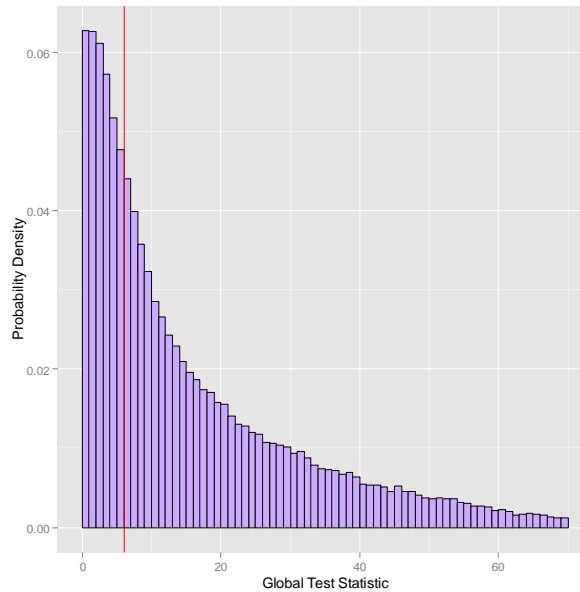


Figure 5 - Distribution of Global Test Statistic from MC simulation with gross errors according to location.

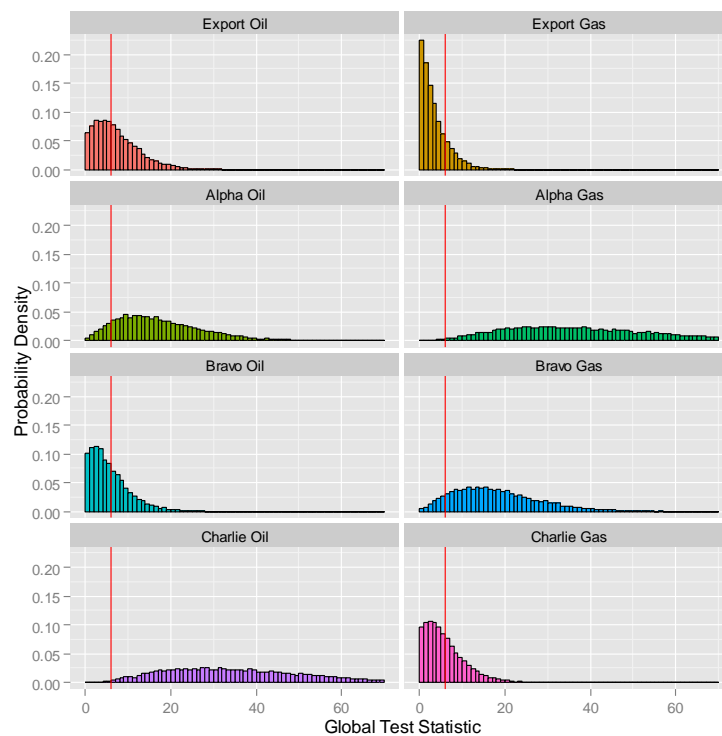


Figure 4 shows the Global Test statistic distribution has a long tail extending far above the critical test threshold, indicating a higher power than the Allocation Factor test

Figure 5 shows that for certain measurements the Global Test statistic is very sensitive to a gross error of the magnitude simulated.

Table 2 quantifies the performance of the Global Test demonstrated in Figure 5 according to the test's AVTI and Power. The first column reports the performance irrespective of the gross error location; subsequent columns indicate the simulated gross error's location

Table 2 - Global Test performance statistics.

| Global Test Error Location | Overall | Export Oil | Export Gas | Alpha Oil | Alpha Gas | Bravo Oil | Bravo Gas | Charlie Oil | Charlie Gas |
|-------------------------------|---------|---------------|---------------|-----------|--------------|-----------|--------------|----------------|----------------|
| Type I Error | 0.048 | 0.051 | 0.045 | 0.045 | 0.045 | 0.047 | 0.056 | 0.040 | 0.057 |
| Power | 0.662 | 0.521 | 0.183 | 0.893 | 0.995 | 0.391 | 0.907 | 0.993 | 0.408 |

AVTI is low for all streams irrespective of gross error location, of the order of 5%, so the possibility of a false alarm is not negligible. Although the overall Power indicates that about 2/3 gross errors would be detected, the Power is much higher than for the Allocation Factor test. The Global Test Power is higher when compared to the Allocation Factor test according to the gross error location, and rises above 90% for some locations.

GLR Test

The GLR Test statistic's probability distribution from the simulation with gross errors is depicted in Figure 6 and according to gross error location in Figure 7. The red vertical line denotes the critical test threshold, the 95% confidence level above which a gross error is detected, $\gamma \geq 7.44$

Figure 6 - Distribution of GLR Test Statistic from MC simulation with gross errors.

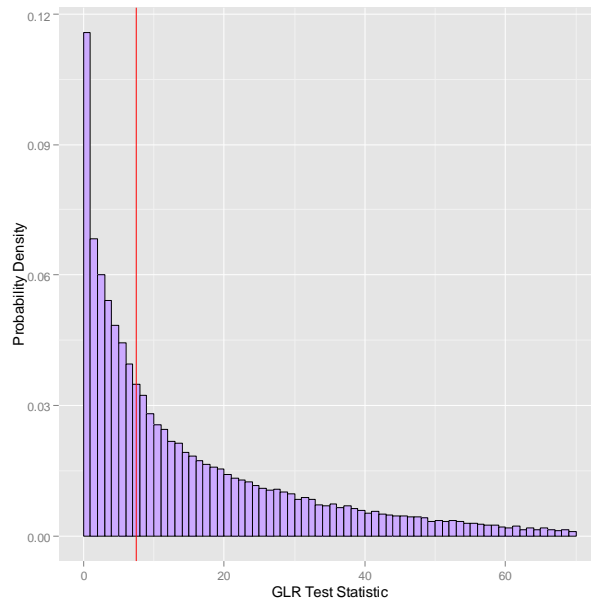
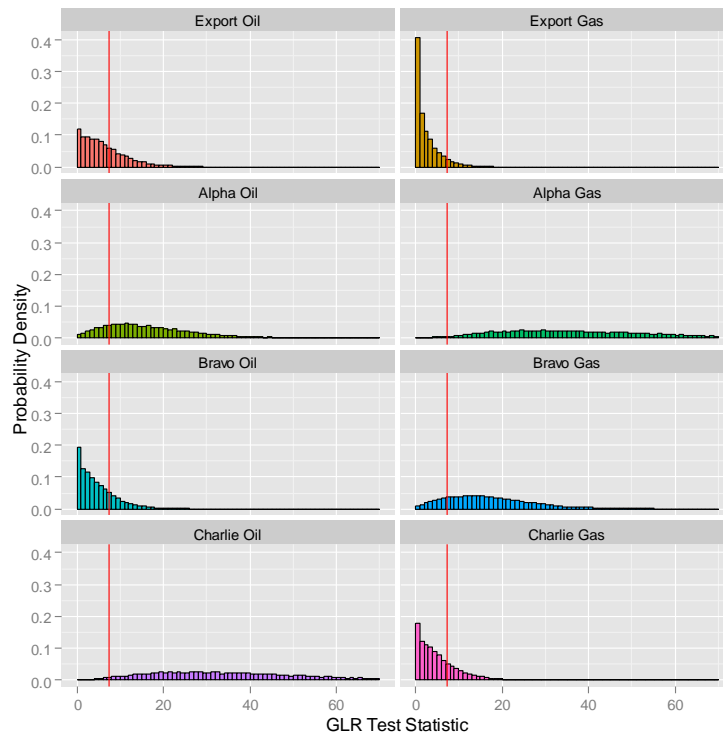


Figure 7 - Distribution of Global Test Statistic from MC simulation with gross errors according to location.



As with the Global Test, Figure 6 shows the GLR Test statistic distribution has a long tail extending far above the critical test threshold, indicating a higher power than the Allocation Factor test

Figure 7 shows that for certain measurements the GLR Test statistic is very sensitive to a gross error of the magnitude simulated.

Table 3 quantifies the performance of the GLR Test demonstrated in Figure 6 according to the test's AVTI and Power.

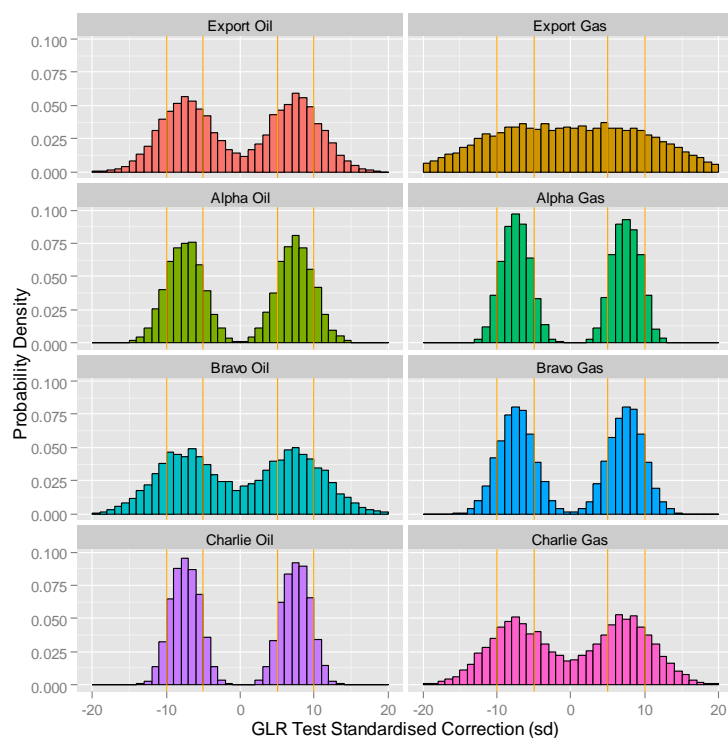
Table 3 - GLR Test performance statistics.

| GLR Test | | | | | | | | | |
|----------------|---------|------------|------------|-----------|-----------|-----------|-----------|-------------|-------------|
| Error Location | Overall | Export Oil | Export Gas | Alpha Oil | Alpha Gas | Bravo Oil | Bravo Gas | Charlie Oil | Charlie Gas |
| Type I Error | 0.006 | 0.007 | 0.003 | 0.010 | 0.006 | 0.004 | 0.008 | 0.003 | 0.007 |
| Power | 0.559 | 0.340 | 0.072 | 0.806 | 0.985 | 0.224 | 0.827 | 0.982 | 0.233 |

AVTI is extremely low for all streams irrespective of gross error location, an order of magnitude lower than for the Global Test, suggesting the possibility of a false alarm is exceedingly unlikely. Although the overall Power indicates that just over half of gross errors would be detected, this is partly due to the low Power for export streams. The test's Power is much higher than for the Allocation Factor test and is higher when compared to the Allocation Factor test according to the gross error location, rising above 90% for some locations.

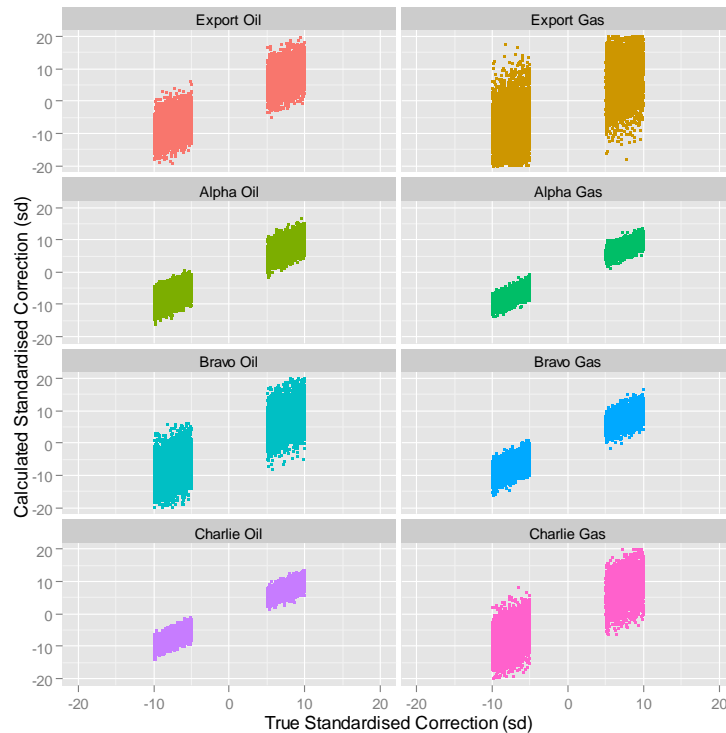
The GLR Test also enables the magnitude of the gross error to be established. Figure 8 shows the distribution of calculated corrections, standardised relative to the measurement uncertainty. The orange vertical lines delineate the range of true values with which gross errors were simulated.

Figure 8 - Distribution of corrections predicted by the GLR test from MC simulation with gross errors according to location



The accuracy with which the GLR Test calculates the value of the gross error varies according to location. The accuracy improves with the test's Power. A scatter plot of calculated correction against the true correction shows the expected correlation.

Figure 9 - Calculated correction predicted by GLR Test plotted against the true gross error.

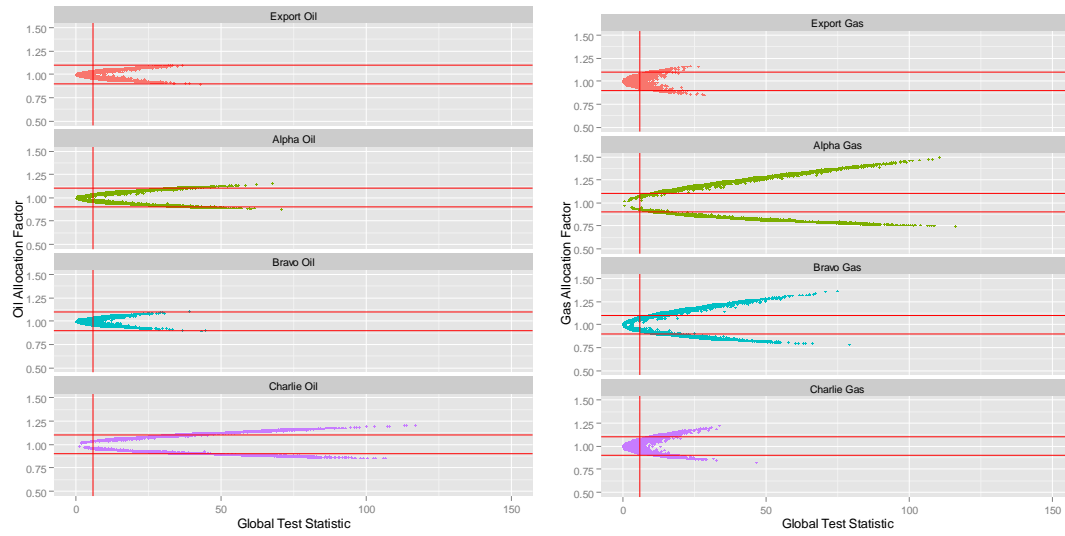


3.3 Comparison of Allocation Factor vs. Global Test

A revealing comparison of the Allocation Factor and Global tests is made in Figure 10. It demonstrates once more the Power of the Global Test in comparison to an Allocation Factor test. The horizontal red lines denote the limits outside of which the Allocation Factor test would identify a gross error. The vertical red line denotes the critical test threshold for the Global Test. For certain gross error locations the Allocation Factor changes slowly in comparison to the Global Test statistic and therefore does not exceed the accepted range for the Allocation Factor test.

Of course, we could revise the accepted range, but in doing so we would have to consider the measurement uncertainties. We would therefore arrive at a position of being able to apply the Global Test, because for the linear case it only requires the measurement data, associated measurement uncertainties and the process constraints. It is not dependent on the results of an allocation system being derived by data reconciliation, pro-rata or even by-difference allocation.

Figure 10 – Scatter plot of Oil and Gas Allocation Factor against Global Test statistic for MC simulation according to gross error location.



4 DESCRIPTION OF GPIII SYSTEM

4.1 Process

A schematic of the sub-sea well configuration is presented in Figure 11:

Figure 11 – Dumbarton, Lochranza and Balloch Sub-Sea Configuration

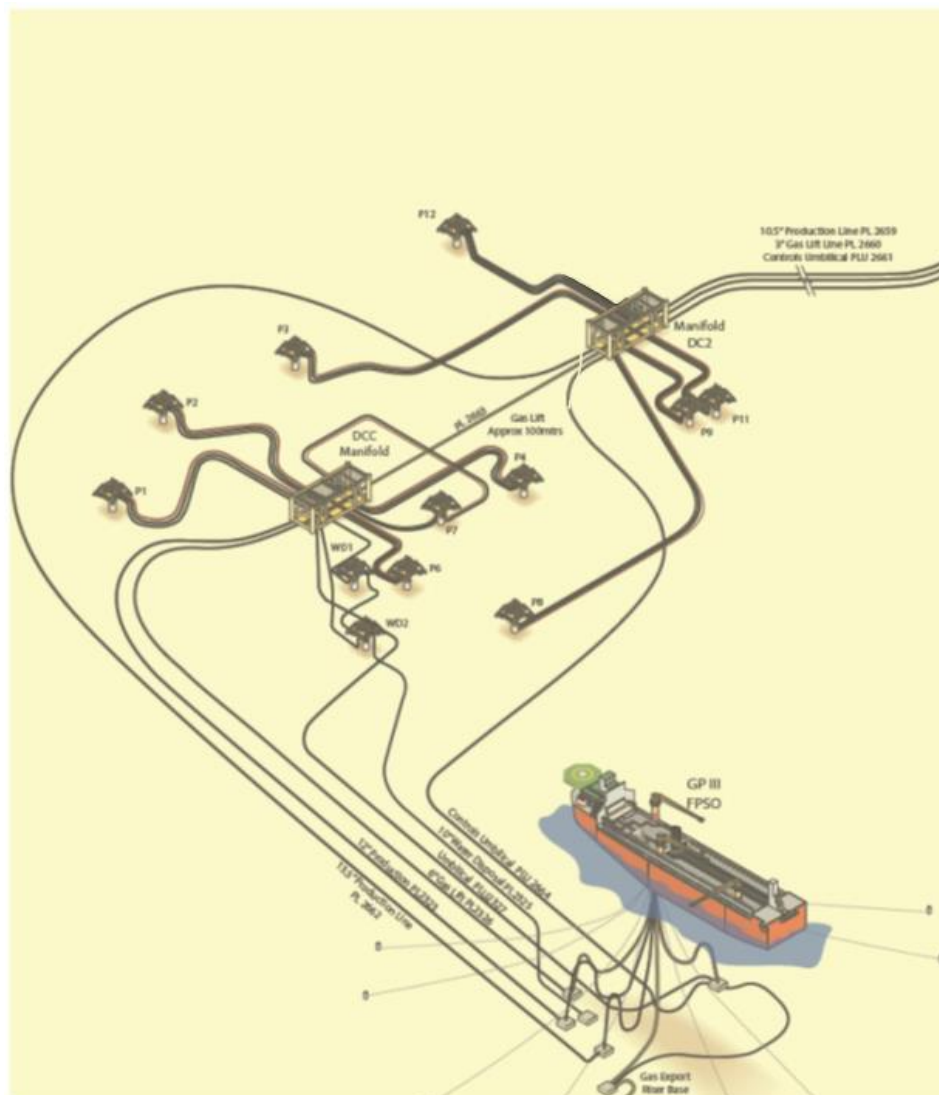
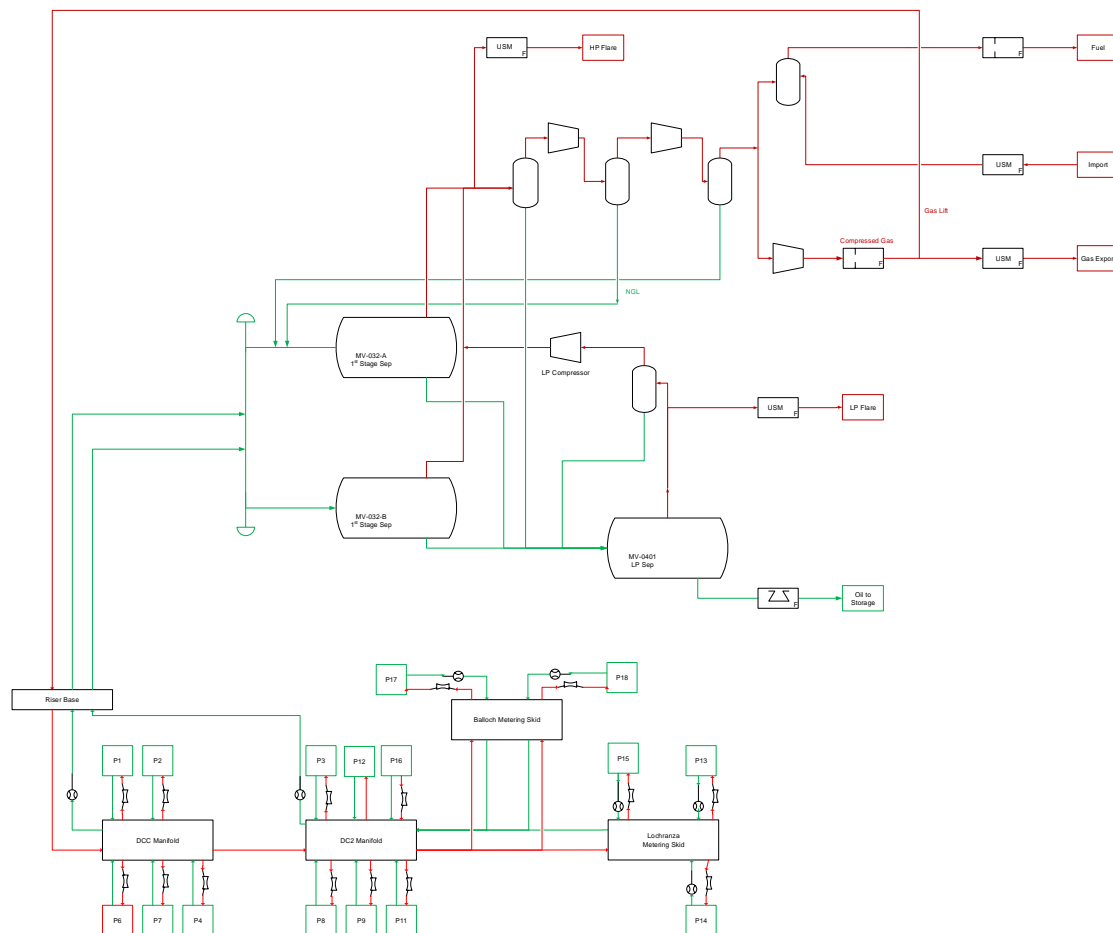


Figure 12 shows the subsea and GPIII topsides process and associated topsides metering:

Figure 12 – GPIII: Simplified Schematic of Subsea and Topsides Process



The GPIII FPSO handles production from the Dumbarton, Lochranza and Balloch fields. Production is metered with a combination of export product meters and subsea multiphase flow meters (MPFM). Each of the Balloch wells and three Lochranza wells have a dedicated MPFM. There is a single MPFM for each of the Dumbarton drill centres (DCC & DC2) which are used to test the performance of the Dumbarton wells and one Lochranza well. Lift gas to each Lochranza well is also individually metered.

As shown in Figure 12, the Dumbarton, Lochranza and Balloch fluids are commingled upstream of the 1st stage separators.

Oil separation on GPIII is achieved using two-stage separation with inlet and 2nd stage heating. Gas from separation is sent to the Low Pressure (LP) and High Pressure (HP) compression trains with produced water passed to the produced water handling package. The plant recycles large quantities of NGL from the compression trains to the separators. This presented difficulties with the modelling of the process in simulation packages as discussed in the earlier paper.

The oil is stabilised, offloaded by tanker and shipped to market. Gas is not currently being exported from GPIII but is utilised as lift and injection gas. Prior to MacCulloch cessation of production, the export gas route was via the MacCulloch FPSO tie-in, onto Piper B and into the Frigg system at St Fergus.

All oil and gas product streams (including fuel and flare) are measured.

4.2 Motivation for Uncertainty Based Allocation

Historically, once Lochranza commenced flowing the Dumbarton field was allocated By-Difference. For example the Dumbarton's allocated oil was determined by subtracting the totalised Lochranza MPFM dry oil flow, after allowing for shrinkage, from the commingled oil export meter.

Similarly, the total produced gas was calculated by summing fuel, flare, export (and netting import) measured flows and subtracting the Lochranza MPFM gas flow, after allowing for lift and process effects, to obtain Dumbarton allocated gas.

This was initially acceptable. However, as indicated in the previous paper, once Dumbarton became the minority field it caused problems with the allocation results; Dumbarton was sometimes allocated oil but not allocated any gas.

One of the key features in the selection of an uncertainty based allocation approach was the identification of the fact that the two fields' wellstream compositions are essentially constant resulting in a stable GOR. Both the Dumbarton and Lochranza reservoir pressures are maintained above the bubble point. This means that the hydrocarbons in the reservoir rock will be in a single phase and hence when produced up the well bore the composition of each field's hydrocarbon fluids entering the GPIII process should be essentially constant. The GOR may vary from day to day depending on operating conditions and any process dynamical instabilities but it should not vary as widely as is observed in the allocated data. Indeed the variation in the allocated GOR has been used as a metric to judge the quality of, and consequently question, the allocation results.

The GORs connect the oil and gas allocated to each field and because they can be estimated to within a tolerance or nominal uncertainty they can be incorporated as inputs into the allocation system. Since the development of GPIII uncertainty based allocation system Balloch has come online. Its reservoir pressure is again above the bubble point and the uncertainty based allocation scheme has been extended to incorporate Balloch.

Mathematical details of the Uncertainty Based Allocation scheme required in this paper are provided in section 8; see the earlier paper [1] for more information.

5 GPIII SIMULATION STUDIES

A similar approach to the MC studies presented in section 3 was undertaken to establish the suitability of the different tests for gross error detection with GPIII. The tests rely on the same concepts used in the GPIII uncertainty based allocation system, with an important addition: the uncertainties in the export gas, export oil, fuel, flare, injection and import gas masses are non-zero allowing them to feature in the GED tests.

The measurement values and relative uncertainties for the MC simulation were taken from a typical recent day. The values shown take into account shrinkage effects. For the purposes of the test they were reconciled to provide a perfect mass balance from which to start the GED tests. Their values and uncertainties are shown in Table 4

Table 4 – Measurement values and uncertainties used in the GPIII MC GED tests

| | Mass or GOR (tonnes or tonnes/tonnes) | Relative Uncertainty (%) |
|-----------------|---|--------------------------------|
| Export Oil | 4556.9 | 1.0% |
| Export Gas | 0.0 | 1.0% |
| Inj Gas | 80.9 | 2.0% |
| Fuel Gas | 6.8 | 5.0% |
| HP Flare Gas | 46.3 | 5.0% |
| LP Flare Gas | 413.1 | 2.0% |
| Import Gas | 0.0 | 1.0% |
| P13 Oil | 0.0 | 0.0% |
| P13 Gas | 0.0 | 0.0% |
| P14 Oil | 138.9 | 21.6% |
| P14 Gas | 12.2 | 128.1% |
| P15 Oil | 252.6 | 29.6% |
| P15 Gas | 22.1 | 179.7% |
| Loch GOR | 0.088 | 56.8% |
| P17 Oil | 1688.1 | 4.6% |
| P17 Gas | 226.8 | 6.0% |
| P18 Oil | 1600.1 | 4.6% |
| P18 Gas | 215.0 | 6.0% |
| Balloch GOR | 0.134 | 57.0% |
| Non-metered Oil | 877.2 | 77.2% |
| Non-metered GOR | 0.081 | 57.1% |

The MPFM uncertainties are affected by both high water cut and uncertainty in the lift gas provided to each well. MPFM uncertainty is initially calculated based on [9] and are in accordance with a GVF below 90% and operating pressure above 20 barg. For an MPFM the dry oil flow uncertainty is function of the measured liquid and WLR and their associated uncertainties. The relative uncertainty in the oil flow is given by:

$$\varepsilon_{M_{Oil}} = \frac{\sqrt{(\varepsilon_{LiQ} * (1 - WLR))^2 + (\varepsilon_{WLR})^2}}{(1 - WLR)} \quad [16]$$

Inspection of the above equation reveals that the relative uncertainty in the oil becomes very large as the WLR approaches 1.

All gas production figures quoted are nett of lift gas. The lift gas metering arrangements require the nett gas production uncertainty at each well to reflect the uncertainties in the Injection Gas meter, individual lift gas meters and subsea MPFM. Propagating these errors leads to the extremely high nett gas production uncertainty on the Lochranza P14 and P15 wells in this example. The Balloch wells do not use lift gas and so their uncertainties are derived from the vendor's datasheet.

The GED tests for GPIII are defined slightly differently to those presented in section 3.1 to take account of the nonlinear constraints.

5.1 Test Definitions

Allocation Factor

The allocation factor for each measurement is defined as, the ratio of allocated mass to measured mass (after taking shrinkage into account), so for example,

$$AF_{P15,Oil} = \frac{am_{P15,Oil}}{m_{P15,Oil}} \quad [17]$$

Where $m_{P15,Oil}$ denotes the P15 MPFM unreconciled shrunk mass of oil and $am_{P15,Oil}$ denotes the mass of oil allocated to P15. We will test for an Allocation Factor in the range $0.9 < AF < 1.1$ as before.

Global Test

Using the Constraint matrix, A , and Jacobian matrix, J , defined for GPIII UBA in section 8 we have approximated the Global Test from linear data reconciliation by calculating the test statistic,

$$\gamma = Ay(JVJ^T)^{-1}(Ay)^T \quad [18]$$

The Constraint and Jacobian matrices used for this paper have been calculated from the unreconciled data. We have assumed that under the null hypothesis the above statistic will approximately follow a χ^2 distribution with four degrees of freedom for the GPIII system under consideration. A gross error is detected if $\gamma \geq \chi^2(\alpha)$, for the chosen confidence level, α . At a 95% confidence level, a gross error is detected if $\gamma \geq 9.49$.

Generalised Likelihood Ratio Test

As earlier, the GLR Test statistic is calculated as:

$$T_k = \frac{d_k^2}{C_k} \quad [19]$$

Where we have approximated the numerator and denominator as

$$d_k = f_k^T (JVJ^T)^{-1} r \quad [20]$$

$$C_k = f_k^T (JVJ^T)^{-1} f_k \quad [21]$$

and each vector f_k is the column of the Jacobian corresponding to the measurement. We have followed the approach in [8] where the Jacobian used in a study of a nonlinear GLR test is that obtained after data reconciliation.

Assuming again that under the null hypothesis the above statistic approximately follows a χ^2 distribution with one degree of freedom a gross error is detected if any of the test statistics exceed the test criterion $\chi^2(\beta)$ for the reduced confidence level where β is given by equation 12. For $\alpha = 0.05$ and with 21 measurements, $\beta = 0.002$. A gross error is then detected if any of the measurement test statistics, $\chi^2(\beta) \geq 9.19$

For the measurement with the highest test statistic above the threshold, the error on that measurement is again estimated according to equation 13.

5.2 Monte Carlo Simulation

A similar Monte Carlo approach to section 3.2 has been taken to analyse expected results for GED tests on GPIII. However, due to the magnitude of some of the measurements' relative uncertainties causing negative simulated unreconciled data only positive gross errors have been simulated. The results are presented in Table 5.

Table 5 – Performance statistics of GED tests applied to GPIII MC simulated data.

| Error Location | Allocation Factor | | Global Test | | GLR Test | |
|-----------------|-------------------|-------|--------------|-------|--------------|-------|
| | Type I Error | Power | Type I Error | Power | Type I Error | Power |
| Overall | 0.215 | 0.273 | 0.060 | 0.544 | 0.006 | 0.420 |
| Export Oil | 0.000 | 0.000 | 0.063 | 0.217 | 0.008 | 0.045 |
| Export Gas | 0.000 | 0.000 | 0.062 | 0.159 | 0.012 | 0.009 |
| Inj Gas | 0.000 | 0.000 | 0.052 | 0.171 | 0.009 | 0.017 |
| Fuel Gas | 0.000 | 0.000 | 0.067 | 0.157 | 0.012 | 0.012 |
| HP Flare Gas | 0.000 | 0.000 | 0.059 | 0.179 | 0.010 | 0.018 |
| LP Flare Gas | 0.000 | 0.000 | 0.056 | 0.289 | 0.011 | 0.092 |
| Import Gas | 0.000 | 0.000 | 0.056 | 0.170 | 0.008 | 0.010 |
| P13 MPFM Oil | 0.000 | 0.000 | 0.060 | 0.162 | 0.006 | 0.009 |
| P13 MPFM Gas | 0.000 | 0.000 | 0.065 | 0.163 | 0.010 | 0.012 |
| P14 MPFM Oil | 0.000 | 0.000 | 0.068 | 0.184 | 0.003 | 0.011 |
| P14 MPFM Gas | 0.939 | 1.000 | 0.060 | 1.000 | 0.003 | 1.000 |
| P15 MPFM Oil | 0.004 | 0.000 | 0.056 | 0.282 | 0.003 | 0.064 |
| P15 MPFM Gas | 0.909 | 1.000 | 0.054 | 0.964 | 0.003 | 0.914 |
| Loch GOR | 0.481 | 0.681 | 0.067 | 0.829 | 0.008 | 0.663 |
| P17 MPFM Oil | 0.000 | 0.000 | 0.055 | 0.808 | 0.004 | 0.613 |
| P17 MPFM Gas | 0.000 | 0.011 | 0.059 | 0.955 | 0.005 | 0.895 |
| P18 MPFM Oil | 0.000 | 0.000 | 0.057 | 0.808 | 0.004 | 0.608 |
| P18 MPFM Gas | 0.000 | 0.009 | 0.059 | 0.952 | 0.004 | 0.886 |
| Balloch GOR | 0.721 | 1.000 | 0.060 | 1.000 | 0.001 | 0.999 |
| Non-metered Oil | 0.786 | 1.000 | 0.062 | 0.998 | 0.003 | 0.997 |
| Non-metered GOR | 0.654 | 1.000 | 0.063 | 0.988 | 0.009 | 0.951 |

Table 5 shows two sides to the use of Allocation Factors to identify errors. For export and disposal streams where the combination of flow rate and measurement uncertainty is low the Type I error rate is found to be zero. However the production streams have high Type I error rates and so the false alarm rate would be high. The Power of the Allocation Factor test is high for several streams. However since these streams are also those where the false alarm rate is high, it seems unlikely that the Allocation Factor test can identify gross errors in the GPIII data without further information.

In contrast, both the Global and GLR tests have respectable Type I error rates irrespective of where a gross error may be located. For certain product streams the Power of the Global and GLR tests are in the region 80 to 90 % indicating good capability to identify gross errors if they do occur.

6 APPLICATION TO GPIII DATA

In light of the MC simulation studies the Allocation Factor test has not been applied to actual GPIII data. The Global and GLR tests have been applied to recent GPIII data and a selection of the results are presented in Figure 13 to Figure 16.

The period had regular stretches of stable production interrupted by occasional upset days. From mid-March to mid-April the Dumbarton P3, Lochranza P15, and Balloch P17 wells were online continuously. From the 9/5 onwards production was again stable with both Balloch wells, the Lochranza P14 and P15 wells and several Dumbarton wells online continuously. Although there are several days during this period when the Global Test indicates a potential gross error, only one day does not coincide with a start-up or shutdown and it seems the most obvious explanation is that the Global Test has raised a false alarm. The GLR Test results are compatible with the Global test.

Figure 13 – Global Test results for March to May 2015

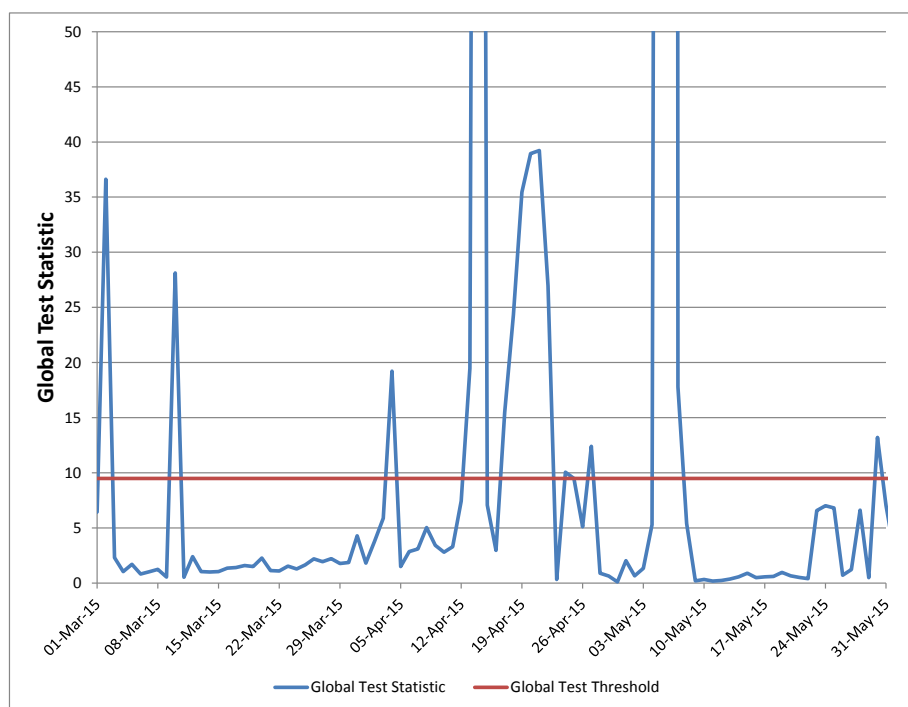


Figure 14 – GLR Test results for Lochranza’s P15 well March to May 2015

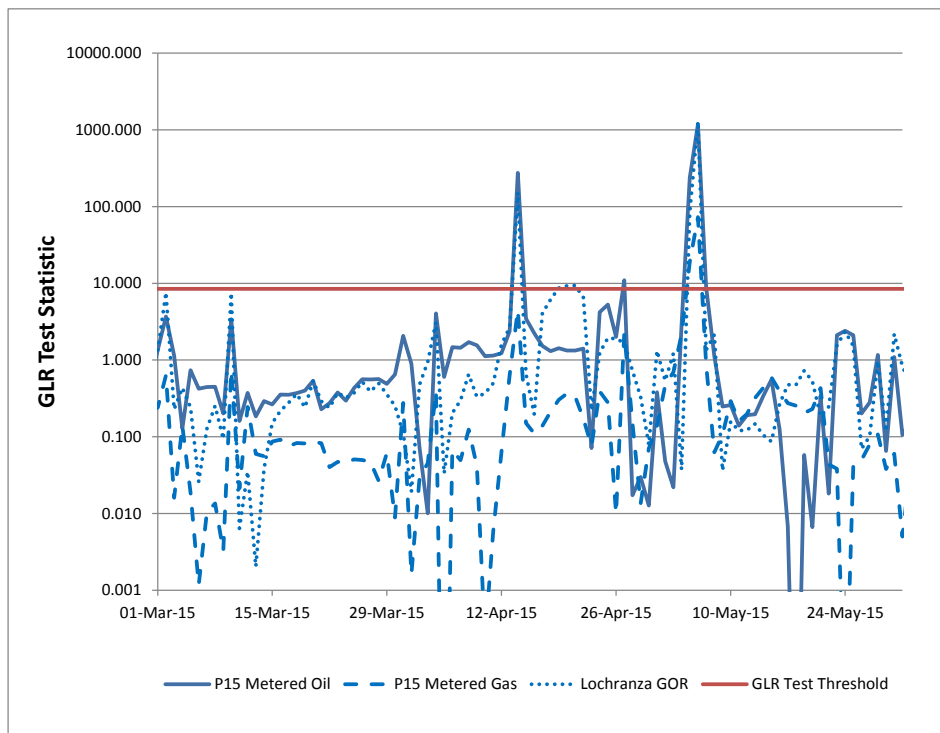


Figure 15 - GLR Test results for Balloch’s P15 well March to May 2015

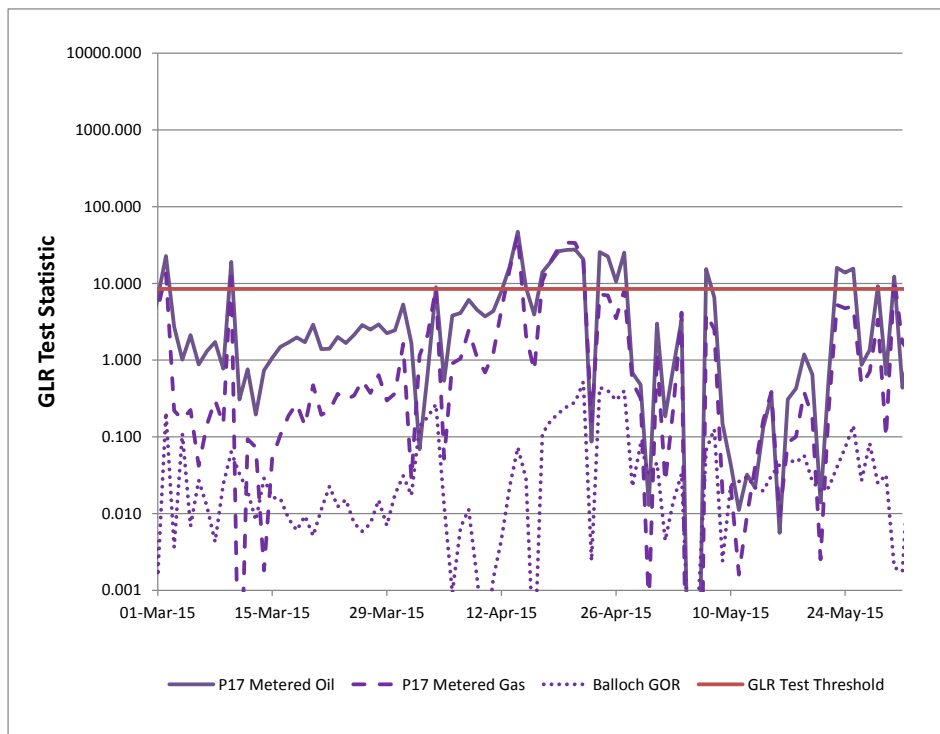
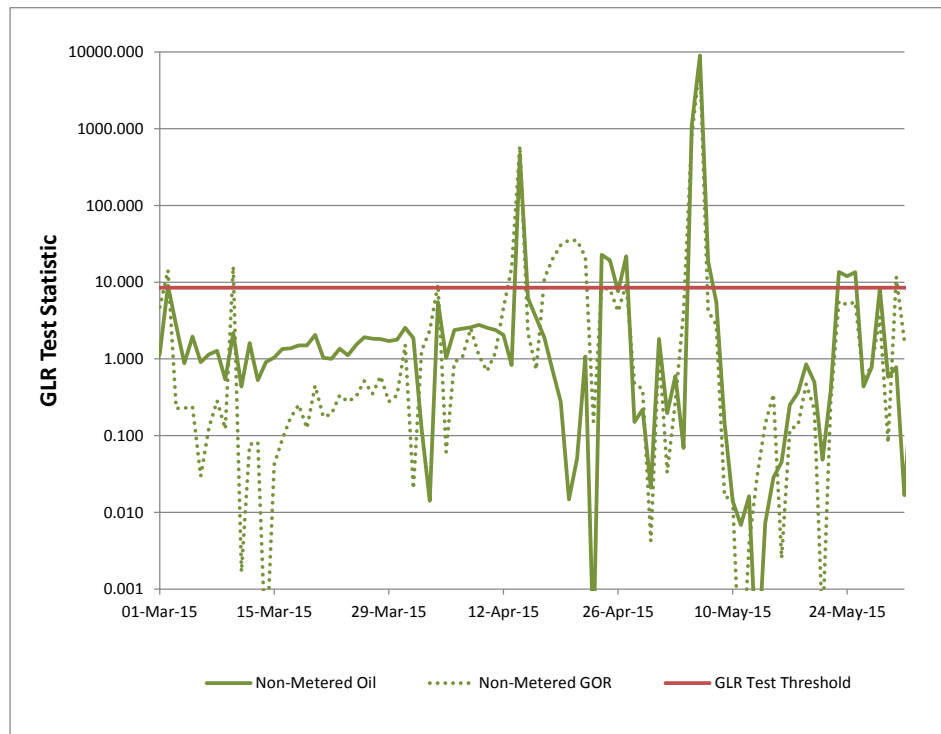


Figure 16 – GLR Test for the non-metered group March to May 2015



7 CONCLUSIONS

The use of Allocation Factors for detecting errors in process data has been compared to the Global and Generalised Likelihood Ratio tests adapted from linear data reconciliation for use in the GPIII UBA system.

Monte Carlo simulation suggests the Global and GLR tests offer a greater chance of accurately identifying gross errors compared to Allocation Factors.

A simple example based on a pro-rata allocation system showed how the Global and GLR tests can be applied to systems which do not implement UBA.

The Global and GLR Tests have been applied to a period of actual GPIII data. Given the assumed uncertainties in measured and estimated quantities, there are relatively few days where the tests identify possible gross errors. The possible gross errors mostly coincide with start-up/shutdown days and are assumed to reflect the non-steady-state nature of these days rather than the presence of gross errors.

8 MATHEMATICAL ANALYSIS UBA MATRIX SOLUTION TECHNIQUE

This section has been taken from [1]. The addition of Balloch wells changes the data reconciliation calculations by requiring an additional gas constraint relating the Balloch gas, oil and GOR. The principles of the UBA approach defined in the following section are otherwise unchanged.

This method is described in [10] and [11] and is based upon the principles of data reconciliation as described more generally in [10].

It should be noted that a rigorous data reconciliation method would reconcile the product measurements (DOILM, EXPGM, etc.) as well as the allocated quantities (ADOILM_g, etc). The sum of allocated quantities would not, therefore, exactly equal the recorded measurements. For allocation, it is generally required that the sum of the allocated quantities is equal to the recorded measurement. So although the product (fiscal) measurements are included in the equations below their uncertainties are assumed to tend to zero, and this ensures the sum of the allocated quantities is equal to the recorded measurement. This is justifiable because the fiscal product measurements are generally substantially more accurate than production estimates.

It should also be noted that total produced gas, with its associated uncertainty, represents the combined fiscal gas export, fuel, flare and injection gas streams less import gas, and their uncertainties. The total produced gas term can be replaced by the individual stream quantities and their associated uncertainties in the following equations. This simply leads to matrices of higher dimension in the equations. The entries representing fiscal export, fuel and flare gas would all be analogous to those for total produced gas shown here. Similarly, water could be included in the data reconciliation, with an additional constraint and inclusion of the necessary metered or estimated stream masses and uncertainties leading to a further increase in the dimensions of the matrices involved in the equations.

Theory

The full system of equations to be solved for the GP III system is shown below:

$$\begin{aligned} \psi = & \left(\frac{ADOILM_{P13} - THWOM_{P13}}{U_{THWOM_{P13}}} \right)^2 + \left(\frac{ADOILM_{P14} - THWOM_{P14}}{U_{THWOM_{P14}}} \right)^2 \\ & + \left(\frac{ADOILM_{P15} - THWOM_{P15}}{U_{THWOM_{P15}}} \right)^2 + \left(\frac{ADOILM_{Dumb} - THWOM_{Dumb}}{U_{THWOM_{Dumb}}} \right)^2 \\ & + \left(\frac{APGASM_{P13} - THWGM_{P13}}{U_{THWGM_{P13}}} \right)^2 + \left(\frac{AGOR_{P14} - THWGM_{P14}}{U_{THWGM_{P14}}} \right)^2 \end{aligned}$$

$$\begin{aligned}
 & + \left(\frac{APGASM_{P15} - THWGM_{P15}}{U_{THWGM_{P15}}} \right)^2 + \left(\frac{AGOR_{Loch} - NOTGOR_{Loch}}{U_{NOTGOR_{Loch}}} \right)^2 \\
 & + \left(\frac{AGOR_{Dumb} - NOTGOR_{Dumb}}{U_{NOTGOR_{Dumb}}} \right)^2
 \end{aligned} \tag{1}$$

The mass balance constraints on the oil phase and gas phase are:

$$\begin{aligned}
 \Phi_{Oil} = 0 = & -DOILM + ADOILM_{P13} + ADOILM_{P14} + ADOILM_{P15} \\
 & + ADOILM_{Dumb}
 \end{aligned} \tag{2}$$

$$\begin{aligned}
 \Phi_{Gas} = 0 = & -TPGASM + APGASM_{P13} + APGASM_{P14} + APGASM_{P15} \\
 & + (ADOILM_{Dumb} * AGOR_{Dumb})
 \end{aligned} \tag{3}$$

$$\begin{aligned}
 \Phi_{Gas} = 0 = & APGASM_{P13} + APGASM_{P14} + APGASM_{P15} \\
 & - (ADOILM_{Loch} * AGOR_{Loch})
 \end{aligned} \tag{4}$$

The optimum solution to the system is found by minimising the value of Ψ (psi) in Equation (1), subject to the constraints of Equations (2), (3) and (4).

For systems with two fields, simultaneous equations can be easily written out explicitly and solved iteratively. However, for systems with more than two fields, the equations are more complex, and a matrix-solution method is recommended. Such a solution is described below.

Matrix Solution Method – Inputs

The input data to the matrix solution method are provided in the form of arrays and vectors. The integer n represents the number of variables to be reconciled.

| | |
|----------|--|
| Y | (Input) vector of measured data (dimension n, 1). |
| X | (Calculated) vector of reconciled data (dimension n,1). |
| V | Variance-covariance matrix for Y (dimension n,n). The covariance of each element to itself is calculated from the square of the absolute uncertainty (U) of the measurement (Y_m) divided by 2, $(U_m/2)^2$. The covariance of any element with any other element is zero because the quantities are independent. |
| J | Jacobian matrix (dimension number of constraint equations n). This contains the coefficients of the derivatives of the oil and gas constraints Equations (2), (3) and (4) – see below for derivation. |

For example, for the 2-field Lochranza and Dumbarton application, the “measured” data comprised the stream measurements and the theoretical oil and gas production (at export conditions) for each Field. These were mass values, based on MPFM measurements for Lochranza Field and on well-tested oil quantities and constant GOR for Dumbarton Field. All theoretical production quantities were calculated within the allocation system.

For a higher-order system, such as GP III, the principles are the same but the matrices are extended to include the additional Field values.

The subsequent matrices are shown with only 2 Fields. Equivalent terms for additional Fields should be inserted where indicated by “...”.

$$Y = \begin{bmatrix} \text{DOILM} \\ \text{TPGASM} \\ \text{THWOM}_{P13} \\ \text{THWGM}_{P13} \\ \dots \\ \text{NOTGOR}_{Loch} \\ \text{THWOM}_{Dumb} \\ \text{NOTGOR}_{Dumb} \end{bmatrix} = \begin{bmatrix} \text{Metered Export Oil} \\ \text{Produced Gas} \\ \text{Theoretical P13 MPM oil (at export conditions)} \\ \text{Theoretical P13 MPM gas (at export conditions)} \\ \dots \\ \text{Notional GOR Lochranza (at export conditions)} \\ \text{Theoretical Dumbarton oil (at export conditions)} \\ \text{Notional GOR Dumbarton (at export conditions)} \end{bmatrix}$$

$$V = \begin{bmatrix} \left(\frac{U_{DOILM}}{2}\right)^2 & 0 & 0 & 0 & \dots & 0 & 0 & 0 \\ 0 & \left(\frac{U_{TPRODGASM}}{2}\right)^2 & 0 & 0 & \dots & 0 & 0 & 0 \\ 0 & 0 & \left(\frac{U_{THWOM,P13}}{2}\right)^2 & 0 & \dots & 0 & 0 & 0 \\ 0 & 0 & 0 & \left(\frac{U_{THWGM,P13}}{2}\right)^2 & \dots & 0 & 0 & 0 \\ \dots & \dots & \dots & \dots & \dots & \dots & 0 & \dots \\ 0 & 0 & 0 & 0 & 0 & \left(\frac{U_{NOTGOR,Loch}}{2}\right)^2 & 0 & 0 \\ 0 & 0 & 0 & 0 & 0 & 0 & \left(\frac{U_{THWOM,Dumb}}{2}\right)^2 & 0 \\ 0 & 0 & 0 & 0 & \dots & 0 & 0 & \left(\frac{U_{NOTGOR,Dumb}}{2}\right)^2 \end{bmatrix}$$

The matrix solution is an iterative method, based on the “Jacobian matrix” (J). The Jacobian terms reflect the non-linear terms in the least-squares-type method used to determine the minimum value of Ψ in Equation (1). The Jacobian terms represent the coefficients of the derivatives of the oil and gas constraints (Equations (2), (3) and (4)) with respect to each reconciled quantity, X_m , e.g., $\partial\Phi_{Oil}/\partial X_m$ and $\partial\Phi_{1Gas}/\partial X_m$.

$$J = \begin{bmatrix} \frac{\partial\Phi_{Oil}}{\partial DOILM} & \frac{\partial\Phi_{Oil}}{\partial TPRODGASM} & \frac{\partial\Phi_{Oil}}{\partial ADOILM_{P13}} & \frac{\partial\Phi_{Oil}}{\partial APGASM_{P13}} & \dots & \dots & \dots & \dots & \frac{\partial\Phi_{Oil}}{\partial AGOR_{Loch}} \\ \frac{\partial\Phi_{1Gas}}{\partial DOILM} & \frac{\partial\Phi_{1Gas}}{\partial TPRODGASM} & \frac{\partial\Phi_{1Gas}}{\partial ADOILM_{P13}} & \frac{\partial\Phi_{1Gas}}{\partial APGASM_{P13}} & \dots & \dots & \dots & \dots & \frac{\partial\Phi_{1Gas}}{\partial AGOR_{Loch}} \\ \frac{\partial\Phi_{2Gas}}{\partial DOILM} & \frac{\partial\Phi_{2Gas}}{\partial TPRODGASM} & \frac{\partial\Phi_{2Gas}}{\partial ADOILM_{P13}} & \frac{\partial\Phi_{2Gas}}{\partial APGASM_{P13}} & \dots & \dots & \dots & \dots & \frac{\partial\Phi_{2Gas}}{\partial AGOR_{Loch}} \end{bmatrix}$$

$$J = \begin{bmatrix} -1 & 0 & 1 & 0 & \dots & \dots & 0 & 1 & 0 \\ 0 & -1 & 0 & 1 & \dots & \dots & 0 & AGOR_{Dumb} & ADOILM_{Dumb} \\ 0 & 0 & AGOR_{Loch} & -1 & \dots & \dots & APGASM_{Loch} & 0 & 0 \end{bmatrix}$$

The matrix solution is therefore an iterative method, because some of the coefficients of the non-linear Jacobian terms ($AGOR_{Dumb}$, $ADOILM_{Dumb}$, $AGOR_{Loch}$ and $ADOILM_{Loch}$) are dependent on the previous solution.

For the first iteration only, the Jacobian matrix uses the theoretical estimates of the non-metered Field GOR and Oil.

Matrix Solution Method

The reconciled measurements X which result in the minimum value of Ψ in the system of equations described above may be described as follows and are calculated using the method described in [10] and shown in Equation (5) below:

$$X = \begin{bmatrix} ADOILM \\ ATPRODGASM \\ ADOILM_{P13} \\ APGASM_{P13} \\ \dots \\ \dots \\ \dots \\ \dots \\ AGOR_{Dumb} \end{bmatrix}$$

$$X = Y - K(f(X_0) + J(Y - X_0)) \quad (5)$$

Where,

\mathbf{X} is the vector containing the reconciled measurements calculated by this iteration.

\mathbf{Y} is the vector containing the initial measurements, as defined above.

\mathbf{K} is an intermediate matrix, defined as:

$$K = VJ^T (JVJ^T)^{-1} \quad (6)$$

\mathbf{V} is the covariance matrix for \mathbf{Y} , as defined above.

\mathbf{J}^T is the transpose of the Jacobian matrix, \mathbf{J} .

$\mathbf{f}(\mathbf{X}_0)$ is the imbalance vector, and is calculated from the product of the Jacobian matrix (\mathbf{J}), and the current estimated measurements (\mathbf{X}_0).

$$f(X_0) = JX \quad (7)$$

\mathbf{J} is the Jacobian matrix, as defined above.

\mathbf{X}_0 is the vector containing the reconciled measurements from the previous iteration.

Matrix Solution Method – Initialisation

1. Specify elements of measurements matrix, \mathbf{Y} .
2. Calculate elements of variance-covariance matrix, \mathbf{V} .
3. Specify initial elements of initial Jacobian matrix, \mathbf{J}_1 , using the theoretical field quantities.
4. Calculate intermediate matrix \mathbf{K} from Equation (6): $\mathbf{K} = \mathbf{V} \mathbf{J}^T (\mathbf{J} \mathbf{V} \mathbf{J}^T)^{-1}$.
5. Initialise value of reconciled measurements vector, $\mathbf{X}_0 = \mathbf{Y}$.
6. Calculate new values of reconciled measurements vector, \mathbf{X} from Equations (5) and (7).

Matrix Solution Method – Iteration

7. Update value of reconciled measurements vector, $\mathbf{X}_0 = \mathbf{X}$ from previous iteration.
8. Update elements of Jacobian matrix, \mathbf{J} , using the latest reconciled measurements.
9. Update intermediate matrix \mathbf{K} from Equation (6): $\mathbf{K} = \mathbf{V} \mathbf{J}^T (\mathbf{J} \mathbf{V} \mathbf{J}^T)^{-1}$.
10. Calculate new values of reconciled measurements vector, \mathbf{X} from Equations 4 and 6.
11. Calculate absolute change in reconciled measurements vector: $\mathbf{ABS}(\mathbf{X} - \mathbf{X}_0)$.
12. If the sum of the absolute changes in reconciled measurements has changed by more than the specified tolerance, repeat steps 7 to 12.

NOTATION

| | | | |
|------------|-------------------------------------|-------------------|---|
| ADOILM | Allocated dry oil mass | X_0 | Reconciled or allocated data from previous iteration vector |
| AGOR | Allocated GOR | Y | Input data vector |
| APGASM | Allocated produced gas mass | Greek | |
| AVTI | Average Type I Error rate | ε | Uncertainty (relative) |
| DOILM | Measured dry product oil mass | θ | Type II Error Rate (1-Power) |
| e | Uncertainty (absolute) | ψ | Objective function |
| EXPGM | Export gas mass | ϕ | Constraint |
| f(X_0) | Imbalance vector | Subscripts | |
| J | Jacobian matrix | Dumb | Dumbarton |
| K | Intermediate matrix | liq | mass of liquid |
| NOTGOR | Notional GOR | Loch | Lochranza |
| P | Constraint projection matrix | moil | mass of oil |
| THWGM | Theoretical well gas mass | P13, etc | Well P13, etc |
| THWOM | Theoretical well oil mass | | |
| TPGASM | Total produced gas mass | | |
| U | Absolute uncertainty | | |
| V | Variance covariance matrix | | |
| WLR | Water Liquid Ratio | | |
| X | Reconciled or allocated data vector | | |

9 REFERENCES

- [1] Allocation in an Uncertain World. Maximising the Use of Data with UBA on Global Producer III, N. Corbett, J. Johnston, R. Sibbald, P. Stockton and A. Wilson, 31st North Sea Flow Measurement Workshop, 22-25 October 2013.
- [2] Ripps, D. L. Adjustment of Experimental Data, Chem. Eng. Prog. Symp. Ser 55, 1965, 61, 8.
- [3] Experiences in the Use of Uncertainty Based Allocation in a North Sea Offshore Oil Allocation System, P. Stockton and A. Spence, Production and Upstream Flow Measurement Workshop, 12-14 February 2008.
- [4] Production Quantification Through Full Field Modelling – Case Study. Kjartan Berg and Daniel Fonnes, 32nd North Sea Flow Measurement Workshop, 21-24 October 2014.
- [5] Data Reconciliation and Gross Error Detection, An Intelligent Use of Process Data, Shankar Narasimhan and Cornelius Jordache, published in 2000 by Gulf Publishing Company, Houston Texas, ISBN 0-88415-255-3.
- [6] Performance Improvement of Large Installation Base of Wellhead Venturi Wet Gas Measurement in Petroleum Development Oman

(PDO). Abdullah Al Obaidani et al., 31st North Sea Flow Measurement Workshop, 22-25 October 2013.

- [7] Determination of Measurement Uncertainty for the Purpose of Wet Gas Hydrocarbon Allocation, R. A. Webb, W. Letton, M. Basil, North Sea Flow Measurement Workshop 2002.
- [8] Renganathan, T. and Narasimhan, S., A Strategy for Detection of Gross Errors in Nonlinear Processes, Ind. Eng. Chem. Res., 1999, 38, 2391.
- [9] Allocation Uncertainty: Tips, Tricks and Pitfalls, Phil Stockton and Allan Wilson, Proceedings of the 30th International North Sea Flow Measurement Workshop, 23-26 October, 2012.
- [10] "Wring more information out of Plant Data", Robert Kneile, Bailey Controls Co, Chemical Engineering March 1995, pps 110 - 116. Box "deriving the SDF" p115, equations (9) and (10).
- [11] The Estimation of Parameters in Nonlinear, Implicit Models, H. I. Britt and R. H. Luecke, Technometrics Vol 15, No.2.